# Phase diagram of QCD

M. A. Halasz,[1] A. D. Jackson,[2] R. E. Shrock,[3] M. A. Stephanov,[3] and J. J. M. Verbaarschot[1]
[1]*Department of Physics and Astronomy, SUNY, Stony Brook, New York 11794*
[2]*The Niels Bohr Institute, Blegdamsvej 17, Copenhagen, DK-2100, Denmark*
[3]*Institute for Theoretical Physics, SUNY, Stony Brook, New York 11794-3840*
(Received 22 April 1998; published 30 September 1998)

We analyze the phase diagram of QCD with two massless quark flavors in the space of temperature $T$ and chemical potential of the baryon charge $\mu$ using available experimental knowledge of QCD, insights gained from various models, as well as general and model independent arguments including continuity, universality, and thermodynamic relations. A random matrix model is used to describe the chiral symmetry restoration phase transition at finite $T$ and $\mu$. In agreement with general arguments, this model predicts a tricritical point in the $T\mu$ plane. Certain critical properties at such a point are universal and can be relevant to heavy ion collision experiments. [S0556-2821(98)01721-4]

PACS number(s): 11.10.Wx, 11.15.Tk, 12.38.Gc, 21.65.+f

## I. INTRODUCTION

Current and projected experimental progress in the physics of heavy ion collisions increasingly demands better theoretical understanding of the underlying phenomena. In particular, the most exciting possibility offered by such experiments is the creation of high temperature and density conditions under which the dynamics of QCD can bring matter into a new state. The challenge is then to calculate the properties of this new phase together with the properties of the phase transition from QCD, the underlying theory of quark-gluon interactions.

Substantial progress has been achieved in our understanding of QCD at high temperature $T$. The foundation of this understanding is provided by lattice field theory Monte Carlo calculations. In particular, we know that in QCD with two massless flavors a transition restoring chiral symmetry occurs at a temperature of approximately 160 MeV [1].

On the other hand, little is known about the behavior of QCD for finite baryon charge density, or chemical potential of the baryon charge $\mu$. Standard lattice Monte Carlo techniques cannot be applied since the determinant of the Dirac operator is complex, and hence the Euclidean path integral defining the theory does not have a Gibbs (i.e., real, positive-definite) measure. A Gibbs measure is needed for the probabilistic interpretation which forms the basis for importance sampling methods such as Monte Carlo calculations. Moreover, the approximation of quenched fermions fails in this case [2,3] for reasons which have been understood recently using the random matrix theory [4]. However, the conditions created in heavy ion collision experiments require an understanding of the regime of high baryon density as well as that of high temperature. As reviewed, e.g., in [5], there is good evidence that central part of the collisions can be described approximately before freeze-out by thermodynamics, so that the temperature and chemical potential can be defined.

The purpose of this paper is to assemble available knowledge about QCD and apply it to the construction of the phase diagram in the $T\mu$ plane. Most of the studies of this phase diagram have concentrated on modeling the properties of the chiral phase transition (see, e.g., [6,7,8,9,10]). In this paper, we present a more complete and less model dependent analysis of the phase diagram which also includes effects from other phase transitions, such as the nuclear matter liquid-gas transition. Naturally, many of the phenomena to be discussed have been studied extensively. As a result, we will repeat some familiar experimental facts and theoretical arguments (with references to some of the original papers or reviews as appropriate). The aim of our analysis is to transform this knowledge into the determination of a phase diagram for QCD in the $T\mu$ plane. Such an analysis is especially important as an extension of Monte Carlo studies, given the technical problems that these encounter with finite baryon charge density.

The chiral phase transition is of primary interest in ultrarelativistic heavy ion experiments since this is the transition that separates the hadronic phase from the quark-gluon phase. In Sec. VI, we introduce a random matrix model of the chiral phase transition at finite $T$ and $\mu$. We find that this model predicts a tricritical point in the $T\mu$ plane in agreement with more generic arguments. We analyze the properties of some thermodynamic observables in the vicinity of this point.

## II. DEFINITIONS

We take as our model the standard approximation in which we (i) consider pure SU(3) QCD with electroweak interactions turned off and (ii) consider this theory with two massless quarks. There is then an exact $SU(2)_L \times SU(2)_R \times U(1)_B$ global symmetry of the action, which is spontaneously broken down to $SU(2)_V \times U(1)_B$ at zero and sufficiently low temperatures by the formation of a condensate, $\langle \bar{\psi}\psi \rangle$. Many features of QCD indicate that this is a reasonable approximation, e.g., the lightness of pions, the success of current algebra relations, etc. (We will comment below on the inclusion of electromagnetic interactions and strange quarks.) This theory is described by a grand canonical partition function which, when written as a path integral, is formally

 

$$Z \equiv e^{-\Omega(T,\mu)/T} = \int \mathcal{D}A \mathcal{D}\bar{\psi} \mathcal{D}\psi \, \exp\{-S_E\}. \tag{1}$$

The Euclidean action $S_E$ is given by

$$S_E = \int_0^{1/T} dx_0 \int d^3x \left[ \frac{1}{2g^2} \mathrm{Tr}\, F_{\mu\nu} F_{\mu\nu} - \sum_{f=1}^{N_f} \bar{\psi}_f \left( \not{\partial} + \not{A} + m_f + \frac{\mu}{N_c} \gamma_0 \right) \psi_f \right], \tag{2}$$

where $N_f = 2$ is the number of flavors, $N_c = 3$ is the number of colors, and $m_f = m = 0$ is the quark mass. The Euclidean matrices $\gamma_\mu$ are Hermitian. Note that with our sign choices positive $m$ and $\mu$ induce positive $\langle \bar{\psi}\psi \rangle$ and $\langle \bar{\psi}\gamma_0\psi \rangle$. The normalization of $\mu$ differs from the normalization customary in lattice calculations by a factor $1/N_c$ (i.e., the baryon charge of a quark). Integrating over the fermion fields we can also write

$$Z = \int \mathcal{D}A \, \exp\left[ -\frac{1}{2g^2} \mathrm{Tr}\, F_{\mu\nu} F_{\mu\nu} \right] \det\left[ \not{D} + m_f + \frac{\mu}{N_c} \gamma_0 \right]. \tag{3}$$

As indicated, this system is characterized by equilibrium values of $T$ and $\mu$. This may be thought of by imagining the system to be in thermodynamic equilibrium with a large reservoir of entropy and baryon charge which is characterized by these values of $T$ and $\mu$. The total energy and baryon charge of our system fluctuate. Of course, the relative magnitude of these fluctuations is negligible for an open system of macroscopic size. The relation between the chemical potential $\mu$ and the average baryon number density (per unit volume) $n$ is the same as that between the temperature $T$ and the average entropy density (per unit volume), $s$:

$$nV = \sum_f \langle \bar{\psi}_f \gamma_0 \psi_f \rangle = -\frac{\partial \Omega}{\partial \mu}, \quad sV = -\frac{\partial \Omega}{\partial T}, \tag{4}$$

where $\Omega$ is the thermodynamic potential defined in Eq. (1). It can also be seen that $\Omega = -pV$, where $p$ is the pressure. In other words, pressure, temperature and chemical potential are not independent variables for our system. Their variations are related by

$$dp = s dT + n d\mu. \tag{5}$$

Both $T$ and $\mu$ (as well as $p$) are intensive parameters. For a system in thermodynamic equilibrium, these quantities are the same for any of its smaller subsystems. In contrast, the extensive densities $s$ and $n$ can differ for two subsystems even when they are in equilibrium with each other. This happens in the phase coexistence region, e.g., a glass containing water and ice. It is more convenient to describe the phase diagram in the space of intensive parameters $T$ and $\mu$. In particular, the first-order phase transition which we shall encounter is characterized by one value of $\mu$ but two values of $n$—the densities of the two coexisting phases. Another reason for working in these coordinates is that first-principle lattice calculations are performed in such a way that $T$ and $\mu$ are the parameters that can be controlled while the densities are measured. The results of relativistic heavy ion collision experiments are also often analyzed using this set of parameters [5].

## III. ZERO TEMPERATURE

We begin by considering the phase diagram as $\mu$ is varied along the line $T = 0$. Strictly speaking, we are not dealing with thermodynamics here since the system is in its ground state. This fact leads to a simple property of the function $n(\mu)$. Let us rewrite the partition function, Eq. (1), as the Gibbs sum over all quantum states, $\alpha$, of the system

$$Z = \sum_\alpha \exp\left\{ -\frac{E_\alpha - \mu N_\alpha}{T} \right\}, \tag{6}$$

where each state is characterized by its energy, $E_\alpha$, and its baryon charge, $N_\alpha$. In the limit $T \to 0$, the state with the lowest value of $E_\alpha - \mu N_\alpha$ makes an exponentially dominant contribution to the partition function. When $\mu = 0$, this is the state with $N = 0$ and $E = 0$, i.e., the vacuum or $\alpha = 0$. Let us introduce

$$\mu_0 \equiv \min_\alpha (E_\alpha / N_\alpha). \tag{7}$$

As long as $\mu < \mu_0$, the state with the lowest of $E_\alpha - \mu N_\alpha$ remains the vacuum, $\alpha = 0$. Therefore, we conclude that, at zero temperature,

$$n(\mu) = 0 \quad \text{for} \quad \mu < \mu_0. \tag{8}$$

What is the value of $\mu_0$? As an exercise, we first consider a free theory of massive fermions carrying one unit of baryon charge. The states which minimize $E_\alpha / N_\alpha$ are states with one or two (more if fermions have flavor or other degeneracy) fermions at rest with $p = 0$. For each of these states, $E_\alpha / N_\alpha = m$, the mass of the fermion. Therefore, $\mu_0 = m$ for such a theory. When $\mu > m$, the ground state is the Fermi sphere with radius $p_F = \sqrt{\mu^2 - m^2}$. Therefore, $n(\mu) = (\mu^2 - m^2)^{3/2}/(3\pi^2)$. Thus, we see that, even in a trivial theory, the function $n(\mu)$ has a singularity at $\mu = \mu_0$. The existence of some singularity at the point $\mu = \mu_0$, $T = 0$ is a robust and model independent prediction. This follows from the fact that a singularity must separate two phases distinguished by an order parameter, e.g., $n$. The function $n \equiv 0$ cannot be continued to $n \neq 0$ without a singularity.

What is $\mu_0$ for the case of QCD, and what is the form of the singularity? The answers to these questions are somewhat different in QCD and in the real world (QCD+) which includes other interactions, most notably electromagnetic interactions. Since QCD is the focus of the present paper and QCD+ is the ultimate goal of our understanding, we shall consider both cases. It is important to understand their differences if we are to extract physically useful predictions from lattice calculations, which are performed for QCD rather than QCD+.

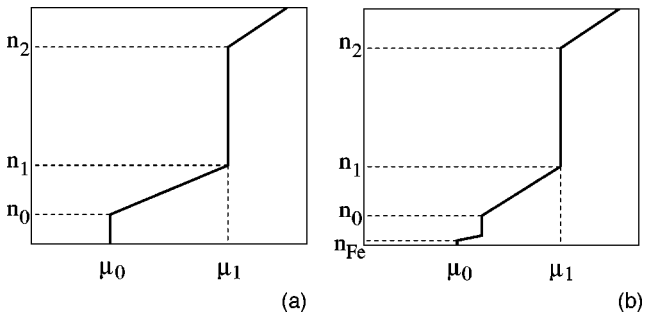


FIG. 1. Schematic dependence of the baryon charge density on the chemical potential at $T=0$ (a) in QCD ($\mu_0 \approx m_N - 16$ MeV) and (b) in QCD+ ($\mu_0 \approx m_N - 8$ MeV).

The energy per baryon, $E/N$, can also be written as $m_N - (Nm_N - E)/N$, where $m_N = m_p \approx m_n$ is the nucleon mass. Therefore, the state which minimizes $E/N$ is that for which the binding energy per nucleon, $\epsilon = (Nm_N - E)/N$, is a maximum. Empirically, we know that this state is a single iron nucleus at rest with $N=A=56$ and $\epsilon \approx 8$ MeV. However, in QCD without electromagnetism the binding energy per nucleon increases with $A$. This is the consequence of the saturation of nuclear forces and can be seen from the Weizsacker formula. Without electromagnetism, only the bulk and surface energy terms are significant for large $A$:

$$\epsilon(A) \equiv \frac{Am_N - m_A}{A} \approx a_1 - a_2 A^{-1/3} \tag{9}$$

with $a_1 \approx 16$ MeV, $a_2 \approx 18$ MeV [11]. As $A \to \infty$, $\epsilon$ saturates at the value $a_1$. This corresponds to the binding energy per nucleon in a macroscopically large sample of nuclear matter as defined by Fetter and Walecka in [11]. We conclude that in QCD the density jumps at $\mu = \mu_0 \approx m_N - 16$ MeV to the value of the nuclear matter density $n_0 \approx 0.16$ fm$^{-3}$. Therefore, in QCD there is a first-order phase transition, characterized by a discontinuity in the function $n(\mu)$ at $\mu = \mu_0$ (see Fig. 1a).

In QCD+, the Coulomb forces change the situation near $\mu_0$. The contribution of the Coulomb repulsion to $\epsilon(A)$ is negative: $-(0.7 \text{ MeV})Z^2/A^{2/3}$, and it is responsible for the experimentally observed maximum in $\epsilon(A)$ at $A \approx 56$. Isospin singlet nuclear matter ($A=\infty$) is unstable at zero pressure due to Coulomb repulsion. Neutron matter with $Z \ll A$ is also unstable at zero pressure, and we are left to consider a gas of iron nuclei. In order to ensure electric neutrality, we must add electrons. Such a gas is clearly unstable at small densities and forms a solid—iron. Therefore, there is a discontinuity in the value of $n(\mu)$ at $\mu_0 \approx m_N - 8$ MeV. This discontinuity is equal to the density of normal matter (i.e., iron) and is about $10^{-14}$ times smaller than in QCD. For very small $\mu - \mu_0$, $n(\mu)$ has structure, fine on the scale of QCD, which reflects the properties of normal matter under pressure. Then, for $\mu - \mu_0 = \mathcal{O}(10-200$ MeV), we traverse the domain of nuclear physics with the possibility for various phase transitions. In particular, a transition to neutron matter ($Z \ll A$) is probably similar to the transition in QCD at $\mu = \mu_0$. (See Fig. 1b.) In this domain, one may encounter such phenomena as nuclear matter crystallization [12,13], superconducting phases of neutron and quark matter [14–16], and, due to the strange quark in QCD+, kaon condensation [12,17] and a transition to strange quark matter [18,19]. Moving along the $\mu$ axis to the right is equivalent to increasing the pressure: $p = \int n d\mu$. Thus, this picture is roughly what one might encounter in moving towards the center of a neutron star from the iron crust at the surface.

Our knowledge of $n(\mu)$ is scanty for densities of order one to ten times $n_0$ and $\mu - \mu_0 = \mathcal{O}(10-200$ MeV) both in QCD and in QCD+. We can only be sure that $n(\mu)$ is a monotonically increasing function, which follows from the requirement of thermodynamic stability.

The behavior of $n(\mu)$ again becomes calculable in the region of very large $\mu \gg \Lambda_{\rm QCD}$. In that case, the Pauli exclusion principle forces the quarks to occupy ever higher momentum states, and, due to asymptotic freedom, the interaction of quarks near the Fermi surface is (logarithmically) weak. The baryon charge density is proportional to the volume of a Fermi sphere of radius $\mu/3$, $n(\mu) \approx N_f(\mu/3)^3/(3\pi^2)$. At low temperatures, only quarks near the Fermi surface contribute to the Debye screening of the gauge fields. The square of the screening mass $m_D^2$ is proportional to the area of the Fermi surface: $m_D^2 \sim g^2\mu^2$. This means that color interactions are screened on lengths $\mathcal{O}(1/g\mu) = \mathcal{O}(\sqrt{\ln(\mu/\Lambda_{\rm QCD})}/\mu)$. This motivates the conclusion that nonperturbative phenomena such as chiral symmetry breaking should be absent at sufficiently large $\mu$. Therefore, in QCD with massless quarks one should expect at least one other phase transition, at a value of $\mu$ which we define as $\mu_1$—a transition characterized by the restoration of the chiral symmetry.

What is the value of $\mu_1$ in QCD, and is it finite? Very little reliable information about the phase transition at $\mu_1$ is available. However, several different approaches agree on the conclusion that the value of $\mu_1$ is finite and that $\mu_1 - \mu_0$ is on the order of the typical QCD scale $\Lambda_{\rm QCD} \approx 200$ MeV$\approx 1$ fm$^{-1}$. For example, equating the quark pressure minus the Massachusetts Institute of Technology (MIT) bag constant to the pressure of nuclear matter yields such an estimate (see, e.g., [20]). Here, we should also point out another interesting distinction between QCD and QCD+: the effect of the strange quark in QCD+ is to decrease the value of $\mu_1$ compared to that of QCD. It has even been conjectured that this effect might be sufficient to drive $\mu_1$ below $\mu_0$, which would make normal nuclear matter metastable [18,19]. Another model which predicts the phase transition at finite $\mu_1$ is the Nambu–Jona-Lasinio model, which focuses on the degrees of freedom associated with the spontaneous chiral symmetry breaking and leads to a similar estimate for $\mu_1$ [9].

What is the order of this phase transition? The MIT bag model predicts that it is a first-order transition since the density $n$ of the baryon charge is discontinuous. Unfortunately, analysis of the Nambu–Jona-Lasinio model shows that the order of the transition depends on the values of parameters, most notably, on the value of the cutoff. A larger cutoff leads to a second-order transition, a smaller cutoff to a first-order

transition [9]. A random matrix model at $T=0$ predicts a first-order phase transition [4]. In this paper, we shall extend the random matrix model to permit consideration of the entire $T\mu$ plane. Before doing this, we shall use more general methods to analyze features of the phase diagram of QCD at finite density *and* temperature in the next section.

An additional, qualitative argument for the first-order nature of the chiral phase transition at $\mu_1$ can also be drawn from a certain analogy of QCD to a metamagnet such as a crystal of ferrous chloride $FeCl_2$. At temperatures below the Néel temperature $T_N$ and at zero magnetic field $H$ such a crystal is antiferromagnetically ordered (i.e., the staggered magnetization $\phi_{\rm st}$ has a nonzero expectation value: $\langle\phi_{\rm st}\rangle \neq 0$). Analogously, $\langle\bar{\psi}\psi\rangle\neq 0$ in QCD below $T_c$. The magnetic field $H$ is not an ordering field for the staggered magnetization because it couples to a different order parameter (i.e., normal magnetization $\phi$ with $\Delta\mathcal{E}=-H\phi$) and induces nonzero $\langle\phi\rangle$. Similarly, the chemical potential induces nonzero $\langle\bar{\psi}\gamma_0\psi\rangle$, and the term $\mu\bar{\psi}\gamma_0\psi$ does not introduce explicit breaking of the chiral symmetry. At some critical value of $H$, ferrous chloride undergoes a first-order phase transition, and the staggered magnetization vanishes: $\langle\phi_{\rm st}\rangle=0$. One could naturally expect that in QCD a similar competition between the low temperature spontaneous ordering $\langle\bar{\psi}\psi\rangle\neq 0$ and the ordering $\langle\bar{\psi}\gamma_0\psi\rangle\neq 0$ induced by $\mu$ would result in a first-order phase transition. This analogy can be continued into the $T\mu$ plane or the $TH$ plane in the case of the antiferromagnet. The antiferromagnet has a well known tricritical point in this plane. Its analogue in QCD will be discussed in Sec. V.

Following the arguments of the two preceding paragraphs, we base our subsequent analysis of the phase diagram of QCD with two massless quarks on the following expectations: (i) $\mu_1\sim\mu_0+\mathcal{O}(200\ \text{MeV})$ and (ii) the transition is of first order.

## IV. FINITE $T$ AND $\mu$

We shall use two order parameters to analyze the phase diagram of QCD at nonzero $T$ and $\mu$: the chiral condensate $\langle\bar{\psi}\psi\rangle$ (per flavor) given by

$$\langle\bar{\psi}\psi\rangle V=-\frac{1}{N_f}\frac{\partial\Omega}{\partial m} \tag{10}$$

and the density of the baryon charge $n$ given by Eq. (4). We have already used $n$ to show that there is a singularity at $\mu=\mu_0$ and $T=0$. It was important for that argument that $n$ be exactly zero for all $\mu<\mu_0$. At nonzero $T$, however, $n$ is not strictly 0 for any $\mu>0$. For example, for very small $\mu$ and $T$ one finds a very dilute gas of light mesons, nucleons and antinucleons with

$$n(T,\mu)\approx\frac{\mu}{T}\left(\frac{2m_NT}{\pi}\right)^{3/2}e^{-m_N/T}. \tag{11}$$

Nevertheless, we can use a continuity argument to deduce that the first-order phase transition at $T=0$, $\mu=\mu_0$ has to remain a first-order phase transition for sufficiently small $T$. Therefore, there must be a line emerging from the point $T=0$, $\mu=\mu_0$. One can think of this transition as boiling the nuclear fluid. The slope of this line can be related to the discontinuities in the entropy density $\Delta s$ (or the latent heat per volume $T\Delta s$) and in the baryon density $\Delta n$ across the phase transition line through the generalized Clapeyron-Clausius relation:

$$\frac{dT}{d\mu}=-\frac{\Delta n}{\Delta s}. \tag{12}$$

This relation follows from the condition that the pressure, temperature and chemical potential should be the same in the two phases on a phase coexistence curve and Eq. (5). In analogy with ordinary liquid-gas transitions, the gaseous phase has a lower particle density (where $\Delta n<0$) and lower entropy density[1] (where $\Delta s<0$). Therefore, the slope $dT/d\mu$ must be negative. We further expect that the slope is infinite at $T=0$ since $s(T=0)=0$, and hence $\Delta s(T=0)=0$. As there is no symmetry-breaking order parameter which distinguishes the two phases, there is no reason why these two phases cannot be connected analytically. As in a typical liquid-gas transition, it is natural to expect that the first-order phase transition line terminates at a critical point with the critical exponents of the three-dimensional Ising model.[2] The temperature of this critical point can be estimated from the binding energy per nucleon in cold nuclear matter, $T_0=\mathcal{O}(10\ \text{MeV})$. (See Fig. 5.) Signatures of this point are seen in heavy ion collisions at moderate energies (i.e., $\approx$1 GeV per nucleon), and the critical properties of this point have been studied through measurements of the yields of nuclear fragments [20,21]. In particular, the reported critical exponents are in agreement with those of the three-dimensional Ising model [21].

Additional phase transitions which might occur at $T=0$ would give rise to additional phase transition lines. One could expect two generic situations. If there is a breaking of a global symmetry (e.g., translational symmetry in the case of nuclear matter crystallization), the phase transition line must separate such a phase from the symmetric phase at higher temperatures without any gaps in the line. Otherwise, the transition can terminate at a critical point.

At very high $T\gg\Lambda_{\rm QCD}$, we have a plasma of quarks and gluons with a logarithmically small effective coupling constant $g(T)$ and we can again calculate the density of the baryon charge $n$:

$$n(T,\mu)\approx 4\int\frac{d^3p}{(2\pi)^3}\left[\exp\frac{|\boldsymbol{p}|-\mu/3}{T}+1\right]^{-1}-\{\mu\rightarrow-\mu\}. \tag{13}$$

[1]The entropy per particle is greater in the gaseous phase, but the entropy per volume $s$ is smaller because of a much smaller particle density.

[2]The Ising nature of the universality class follows from the fact that the transition can be modeled by an Ising lattice gas.

We expect that the chiral condensate is zero at very high $T$ since the effective coupling is weak because of asymptotic freedom. Therefore, a phase transition must separate the quark gluon phase from the low temperature phase. This transition has been studied extensively at $\mu=0$ using a variety of methods. In particular, lattice calculations have established the value of $T_c$ as approximately 160 MeV [1]. Arguments based on universality suggest that this transition is of second order with critical exponents of the $SU(2)_L \times SU(2)_R \sim O(4)$ universality class [22]. Lattice calculations seem to confirm this scenario [23].[3] Here, we assume that this is the case and try to understand what happens to this transition when $\mu$ is not zero.

For massless quarks, the low-temperature hadronic phase and the quark-gluon plasma phase can be distinguished by the expectation value of $\langle\bar{\psi}\psi\rangle$, since this is identically zero in the quark-gluon phase and nonzero in the hadronic phase with spontaneously broken chiral symmetry. Therefore, when quark masses are strictly zero, a phase transition must separate these two phases, i.e., these phases cannot be connected analytically in the $T\mu$ plane at $m=0$. Therefore, a line of phase transitions must begin from the point $T=T_c$, $\mu=0$ and continue into the $T\mu$ plane.

As discussed above, chiral symmetry restoration at $T=0$ is most likely to proceed via a first-order phase transition. Therefore, the transition must remain first-order as we continue along a line into the $T\mu$ plane. The slope of this line can again be related to the discontinuity in the baryon charge and the entropy density (12). Since we expect that both density and entropy will be larger in the quark-gluon phase, the slope of this line, $dT/d\mu$, should be negative.

This first-order transition line cannot terminate because the order parameter $\langle\bar{\psi}\psi\rangle$ is identically zero on the one side of the transition. The minimal possibility is that it merges with the second-order phase transition line coming from $T=T_c$, $\mu=0$; the point where the two lines join is a tricritical point [6,7,9]. Such a point exists in many physical systems (e.g., in the $FeCl_2$ antiferromagnet), and universal behavior in the vicinity of this point has been studied extensively. In the next section, we review those properties of a tricritical point which follow from universality.

## V. UNIVERSAL PROPERTIES OF THE TRICRITICAL POINT

By analogy with an ordinary (bi)critical point, where two distinct coexisting phases become identical, one can define the tricritical point as a point where three coexisting phases become identical simultaneously. A tricritical point marks an end-point of three-phase coexistence. In order to see this in QCD, it is necessary to consider another dimension in the space of parameters—the quark mass $m$. This parameter breaks chiral symmetry explicitly. In such a three-dimensional space of parameters, one can see that there are two surfaces (symmetric with respect to $m\rightarrow -m$ reflection) of first-order phase transitions emanating from the first-order line at $m=0$. On these surfaces or wings with $m\neq 0$, two phases coexist: a low density phase and a high density phase. There is no symmetry distinguishing these two phases since chiral symmetry is explicitly broken when $m\neq 0$. Therefore, the surfaces can have an edge which is a line of critical points. These lines, or wing lines, emanate from the tricritical point. The first-order phase transition line can now be recognized as a line where three phases coexist: the high $T$ and density phase and two low density and $T$ phases with opposite signs of $m$ and, hence, also of $\langle\bar{\psi}\psi\rangle$. This line is called, therefore, a triple line.

The plane $m=0$ is a symmetry plane. Chiral symmetry is exact only in this plane, and it is only here that the low and the high temperature phases must be separated by a transition. One can also view this plane as a first-order phase transition surface, since $\langle\bar{\psi}\psi\rangle$ has a discontinuity across it. Then, the second-order phase transition line together with the triple line provide a boundary for this surface.

Critical behavior near the tricritical point can now be inferred from universality. The upper critical dimension for this point is 3. Since critical fluctuations are effectively three-dimensional for the second-order phase transition at finite $T$, we conclude that behavior near this point is described by mean field exponents with only logarithmic corrections. The effective Landau-Ginsburg theory for the long-wavelength modes $\phi\sim\langle\bar{\psi}\psi\rangle$ near this point requires a $\phi^6$ potential which has the form (in the symmetry plane $m=0$)

$$\Omega_{\rm eff}=\Omega_0(T,\mu)+a(T,\mu)\phi^2+b(T,\mu)\phi^4+c(T,\mu)\phi^6 \tag{14}$$

with $c>0$. The $\phi^6$ term is necessary in order to create three minima corresponding to the three coexisting phases. This explains why the critical dimensionality is 3, since for this dimension, the operator $\phi^6$ becomes a marginal operator. When $b>0$, the transition occurs when $a=0$ and is a second-order transition similar to that seen in a $\phi^4$ theory. This corresponds to the second-order line. When $b<0$ the transition occurs at some positive value of $a$ and is of first order. This is the triple line. When both $a$ and $b$ vanish, we have a tricritical point.

In particular, the following exponents in the symmetry plane $m=0$ are readily found using mean field $\phi^6$ theory (as noted above, renormalization group studies [25] show that the actual singularities include additional, logarithmic corrections). The discontinuity in the order parameter $\langle\phi\rangle=\langle\bar{\psi}\psi\rangle$ along the triple line as a function of the distance from the critical point $\mu_3, T_3$ (measured either as $T_3-T$ or $\mu-\mu_3$) behaves like

$$\Delta\langle\bar{\psi}\psi\rangle\sim(\mu-\mu_3)^{1/2}. \tag{15}$$

The discontinuity in the density $n=d\Omega_{\rm eff}/d\mu$ across the triple line behaves like

[3] A sufficiently light third quark would drive the transition first-order [22]. However, lattice calculations of the Columbia group [24] using staggered fermions indicate that the strange quark is not sufficiently light for this to occur. This issue has also been studied using Wilson fermions, although in this case one must tune the action to counteract the explicit chiral symmetry breaking that it introduces even for massless quarks; see Iwasaki *et al.* in Ref. [24].

$$\Delta n \sim (\mu - \mu_3)^1. \tag{16}$$

The critical behavior along the second-order line is everywhere the same as at the point $\mu = 0$, $T = T_c$ (which is an infrared attractive fixed point). Therefore, $\langle \bar{\psi}\psi \rangle$ vanishes on the second-order line with $O(4)$ exponents. At the tricritical point, however, the exponent with which $\langle \bar{\psi}\psi \rangle$ vanishes is given by the Landau-Ginzburg theory as

$$\langle \bar{\psi}\psi \rangle \sim (T_3 - T)^{1/4}. \tag{17}$$

When $m \neq 0$, the potential $\Omega_{\rm eff}(\phi)$ can also contain terms $\phi$ and $\phi^3$ which break $\phi \rightarrow -\phi$ symmetry explicitly. (The term $\phi^5$ can be absorbed by a shift of $\phi$.) The potential $\Omega_{\rm eff}(\phi)$ still has three minima, and a first-order phase transition can occur when two adjacent minima are equally deep. These transitions form a surface of first-order phase transitions—the wings. The two minima (and an intermediate maximum) can also fuse into a single minimum. This happens on the wing lines at the edge of the surface of first-order phase transitions. The critical behavior along the wing lines is given by the three-dimensional Ising exponents, as is usual at the endpoints of first-order liquid-gas type phase transitions not associated with restoration of a symmetry. In particular, the discontinuity in $\Delta\langle \bar{\psi}\psi \rangle$ and $\Delta n$ vanishes with exponent $\beta \approx 0.31$. These discontinuities are related to the slope of the wing surface at constant $T$ through a relation similar to Eq. (12):

$$\frac{d\mu}{dm} = -\frac{\Delta\langle \bar{\psi}\psi \rangle N_f}{\Delta n}. \tag{18}$$

There are many other universal properties in the vicinity of a tricritical point which can be derived from the above $\phi^6$ Landau-Ginzburg effective potential. One can, for example, show that the $m = 0$ second-order line, the wing lines, and the triple lines approach the triple point with the same tangential direction: The second-order line approaches from one side while the wing lines and the triple line approach from the opposite side. For a more detailed description of the properties of tricritical points, see Ref. [25].

## VI. A RANDOM MATRIX MODEL AT FINITE $T$ AND $\mu$

Random matrix models have proven to be a valuable tool for studying spontaneous chiral symmetry breaking in QCD. For example, it has been conjectured that the distribution of the eigenvalues of the Dirac operator near zero is universal [26]. The universal expressions show a remarkable agreement with lattice Monte Carlo data [27] and are consistent with spectral sum rules from chiral perturbation theory [26]. Random matrix models have also been used to study chiral symmetry restoration phenomenon at finite temperature [28–30] as well as finite chemical potential [4,31–33].

Random matrix theory provides an effective description of those degrees of freedom in QCD which are responsible for the spontaneous breaking of chiral symmetry. In this respect, it is similar to Landau-Ginzburg effective theory. Random matrix theory is based on the observation that the spontaneous chiral symmetry breaking is related to the density of small eigenvalues of the Dirac operator ($\lambda \ll \Lambda_{\rm QCD}$). This relationship is expressed quantitatively by the Banks-Casher formula [34], $\langle \bar{\psi}\psi \rangle = \pi \rho_{\rm ev}(0)$. Here, $\rho_{\rm ev}(0)$ is the density of small (but non-zero) eigenvalues (per unit $\lambda$ and per unit four-volume, $V_4$) of the Euclidean Dirac operator in the thermodynamic limit $V_4 \rightarrow \infty$. The dynamics of these eigenvalues can be described using a random matrix (of infinite size) in place of the Dirac operator. This approximation can be shown to give exact results in the mesoscopic limit [26,35].

When the chemical potential is non-zero, the Dirac operator is not Hermitian, and its determinant is no longer real. As a result, the density of its eigenvalues can be defined straightforwardly only in quenched QCD, i.e., when the contribution of the (complex) fermion determinant to the measure is approximated by unity. Fortunately, a more general relation exists between the chiral condensate and the linear density of zeroes of the partition function:

$$\langle \bar{\psi}\psi \rangle = \pi \rho(0). \tag{19}$$

As observed by Yang and Lee [36], non-analytic behavior in a thermodynamic quantity, including in the present case the discontinuity in the value of an order parameter in the thermodynamic limit, is caused by the coalescence of zeros of the partition function to form a boundary crossing the relevant parameter axis. In the case of QCD, the signature of spontaneous chiral symmetry breaking is the discontinuity in $\langle \bar{\psi}\psi \rangle$ as $m$ is varied along the real axis and crosses $m = 0$. This discontinuity is equal to $2\pi\rho(0)$ where $\rho(0)$ is the density of the zeroes on the imaginary $m$ axis near $m = 0$ in the thermodynamic limit. One can also show that $\rho \rightarrow \rho_{\rm ev}$ in the quenched limit $N_f \rightarrow 0$ but *only* when $\mu = 0$. For nonzero $\mu$, the density of the eigenvalues, $\rho_{\rm ev}$, is fundamentally different from the $N_f \rightarrow 0$ limit of $\rho$ [4].

It can be shown that certain properties of the small eigenvalues of the Dirac operator are universal and are identical to those of a random matrix model with appropriate symmetries [37–39,35,27,40]. The virtue of the random matrix model is that it is solvable, i.e., one can calculate the distribution of the eigenvalues and of the Yang-Lee zeroes. The partition function of QCD at finite temperature and chemical potential in random matrix approximation is given by

$$Z_{\rm RM} = \int \mathcal{D}X \, \exp\left( -\frac{N}{\sigma^2} \, {\rm Tr} \, XX^\dagger \right) {\rm det}^{N_f}(D + m), \tag{20}$$

where $D$ is the $2N \times 2N$ matrix approximating the Dirac operator $\not{D} + (\mu/N_c)\gamma_0$:

$$D = \begin{pmatrix} 0 & iX + iC \\ iX^\dagger + iC & 0 \end{pmatrix}. \tag{21}$$

The random matrix $X$ has dimension $N \times N$. The total dimension of $D$ is $2N$. This is the number of small eigenvalues, which is proportional to $V_4$. In QCD we expect $N$ to be approximately equal to the typical number of instantons (or anti-instantons) in $V_4$; therefore, $N/V_4 \approx n_{\rm inst} \approx 0.5$ fm$^{-4}$ [41]. The matrix $C$ is deterministic and describes the effects

of temperature and chemical potential. In the simplest (and original) $T\neq 0$, $\mu=0$ model [28], the choice $C=\pi T$ describes the effect of the smallest Matsubara frequency. As noted in Ref. [30], it is possible to simulate the effects of the eigenvalue correlations induced by the pairing of instantons and anti-instantons into molecules by choosing a more general form for the diagonal matrix $C$ with elements $C_k$ which are (increasing) functions of $T$. In the $T=0$, $\mu\neq 0$ model of Ref. [4], $C=\mu/(iN_c)$ describes the effect of the chemical potential. In this paper, we consider the more general case $T\neq 0$, $\mu\neq 0$. Although we do not know the detailed dependence of the elements of $C$ on $T$ and $\mu$, we understand that $T$ primarily affects the real (i.e., Hermitian) part of $C$ and $\mu$ affects the imaginary (i.e., anti-Hermitian) part. We shall adopt the following approximate form for this dependence, $C_k=a\pi T+b\mu/(iN_c)$ for one half of eigenvalues and $C_k=-a\pi T+b\mu/(iN_c)$ for the other half with $a$ and $b$ dimensionless parameters.[4] This form accounts for the fact that there are the two smallest Matsubara frequencies,[5] $+\pi T$ and $-\pi T$. Such a linear ansatz for $C$ is certainly very naive, but in this paper we decided not to try to refine it. This form reflects sufficiently well our understanding of the properties of $C$.

The chiral condensate is calculated as

$$\langle\bar{\psi}\psi\rangle=\frac{1}{N_f V_4}\frac{\partial \ln Z_{\rm RM}}{\partial m}. \tag{22}$$

Current algebra fixes the value of $\langle\bar{\psi}\psi\rangle_0\approx 2\ \mathrm{fm}^{-3}$ at $T=\mu=m=0$. The only dimensionful parameter remaining in the partition function $Z_{\rm RM}$ is the variance of the random matrix, $\sigma$. Thus,

$$\langle\bar{\psi}\psi\rangle_0=\text{const}\times\frac{N}{V_4\sigma}\approx\text{const}\times\frac{n_{\rm inst}}{\sigma}. \tag{23}$$

The dimensionless constant will be found below and is equal to 2. This fixes the value of $\sigma\approx 0.5\ \mathrm{fm}^{-1}\approx 100$ MeV. It is convenient to use $\sigma$ as a unit of mass in the model and also absorb the coefficients $\pi a$ and $b/N_c$ into $T$ and $\mu$. In other words, we measure $m$ in units of $\sigma$, $T$ in units of $\sigma/(\pi a)$ and $\mu$ in units of $\sigma N_c/b$.

The $N\to\infty$ (i.e., thermodynamic) limit of the partition function, Eq. (20), can be found in the now-standard way [28–30]. Performing the Gaussian integration over $X$ and introducing auxiliary $N_f\times N_f$ matrices $\phi$, one can rewrite the partition function in the form

$$Z_{\rm RM}=\int \mathcal{D}\phi\ \exp[-N\ \mathrm{Tr}(\phi\phi^\dagger)]\det{}^{N/2}\begin{pmatrix}\phi+m & \mu+iT\\ \mu+iT & \phi^\dagger+m\end{pmatrix}\det{}^{N/2}\begin{pmatrix}\phi+m & \mu-iT\\ \mu-iT & \phi^\dagger+m\end{pmatrix}=\int \mathcal{D}\phi\ \exp[-N\Omega(\phi)], \tag{24}$$

where

$$\Omega(\phi)=\mathrm{Tr}[\phi\phi^\dagger-\tfrac{1}{2}\ \ln\{[(\phi+m)(\phi^\dagger+m)-(\mu+iT)^2]\cdot[(\phi+m)(\phi^\dagger+m)-(\mu-iT)^2]\}]. \tag{25}$$

The integration in Eq. (24) is performed over $2\times N_f\times N_f$ variables which are the real and imaginary parts of the elements of the complex matrix $\phi$. In the limit $N\to\infty$ this integral is determined by a saddle point of the integrand or, alternatively, the minimum of $\Omega(\phi)$:

$$\lim_{N\to\infty}\frac{1}{N}\ln Z_{\rm RM}=-\min_{\phi}\Omega(\phi). \tag{26}$$

The function $\Omega(\phi)$ is an effective potential for the degrees of freedom describing the dynamics of the chiral phase transition. One can see that the value of $\phi$ at the minimum, i.e., the equilibrium value $\langle\phi\rangle$, gives us the value of the chiral condensate, Eq. (22):

$$\langle\bar{\psi}\psi\rangle=\frac{1}{N_f V_4}\frac{N}{\sigma}\,2\ \mathrm{Re}\ \mathrm{Tr}\langle\phi\rangle, \tag{27}$$

[cf. Eq. (23)].

For real $m$, it is reasonable to expect that the minimum occurs when $\phi$ is a real matrix proportional to a unit matrix. With this assumption, we need to find only one real parameter, $\phi$, which minimizes the potential:

$$\Omega=N_f\left[\phi^2-\frac{1}{2}\ln\{[(\phi+m)^2-(\mu+iT)^2]\cdot[(\phi+m)^2-(\mu-iT)^2]\}\right]. \tag{28}$$

This is not a simple $\phi^6$ potential, but it has remarkably similar properties. In particular, the condition $\partial\Omega/\partial\phi=0$ gives a fifth-order polynomial equation in $\phi$. Let us first consider the symmetry plane $m=0$. Then the equation $\partial\Omega/\partial\phi=0$ always has one trivial root, $\phi=0$. The remaining four roots are the solutions of a quartic equation, which has the form of a quadratic equation in $\phi^2$:

[4]These parameters are intended to reflect the degree of overlap and correlation between instantons and anti-instantons. One can therefore anticipate that $a$ and $b$ are smaller than 1. We shall estimate the values of $a$ and $b$ below.

[5]Alternatively, this form preserves the relation $\langle\gamma_0 D\rangle=0$ at $\mu=0$.

$$\phi^4 - 2\left(\mu^2 - T^2 + \frac{1}{2}\right)\phi^2 + (\mu^2 + T^2)^2 + \mu^2 - T^2 = 0. \tag{29}$$

Above the second-order line, i.e., in the high temperature phase, Eq. (29) does not have real roots (since $\phi^2 < 0$ for each pair of roots). This corresponds to the fact that the potential $\Omega$ has only one minimum at $\phi = 0$ (i.e., the trivial root). On the second-order line, a pair of roots of Eq. (29) becomes zero, i.e., the potential is $\Omega \sim \phi^4$ near the origin. This means that on the second-order line,

$$(\mu^2 + T^2)^2 + \mu^2 - T^2 = 0. \tag{30}$$

The second-order line ends when the remaining pair of roots also becomes zero, i.e., the potential becomes $\Omega \sim \phi^6$ near the origin. This happens when

$$\mu^2 - T^2 + \frac{1}{2} = 0 \tag{31}$$

on the second-order line. The condition, Eq. (31) together with Eq. (30) determines the location of the tricritical point in the $T\mu$ plane:

$$T_3 = \frac{1}{2}\sqrt{\sqrt{2}+1} \approx 0.776 \quad \text{and} \quad \mu_3 = \frac{1}{2}\sqrt{\sqrt{2}-1} \approx 0.322. \tag{32}$$

The equation for the triple line is obtained from the requirement that the depth of the minima in $\Omega$ at $\phi$ given by the pair of solutions of Eq. (29) (farthest from the origin) should coincide with the depth at the origin $\phi = 0$. The equation for the triple line is therefore

$$\mu^2 - T^2 + \frac{1}{2} + \frac{1}{2}\sqrt{1 - 16\mu^2 T^2} - \frac{1}{2}\ln\left(\frac{1 + \sqrt{1 - 16\mu^2 T^2}}{2}\right) + \ln(\mu^2 + T^2) = 0. \tag{33}$$

In particular, when $T = 0$, we obtain the elementary equation $\mu^2 + 1 + \ln \mu^2 = 0$ whose solution is $\mu \approx 0.528$ [4]. This is the value of $\mu_1$. Setting $\mu = 0$ in the equation for the second-order line, Eq. (30), we find $T_c = 1$ [28].

We recall that the units of $T$ and $\mu$ depend on the unknown dimensionless parameters $a$ and $b$. However, these unknown factors cancel from the ratios

$$\frac{T_3}{T_c} \approx 0.78, \quad \frac{\mu_3}{\mu_1} \approx 0.61. \tag{34}$$

Taking $T_c = 160$ MeV and $\mu_1 = 1200$ MeV, we find that $T_3 \approx 120$ MeV and $\mu_3 \approx 700$ MeV.[6]

Note that the second-order line, Eq. (30), marks the location of the points on the phase diagram where the symmetric minimum $\phi = 0$ disappears, i.e., turns into a maximum. Continuing this line below point $T_3$, we obtain the location of spinodal points. In the region between this line of spinodal points and the first-order phase transition line, the chirally symmetric phase $\phi = 0$ can exist as a metastable state. Such a state can be reached by supercooling, and it is unstable towards the nucleation of bubbles of the broken phase $\phi \neq 0$. A similar line with equation $4T\mu = 1$, the superheating line, together with the supercooling line, Eq. (30), bound the region around the first-order phase transition line where the potential $\Omega(\phi)$ has 3 minima. All these lines meet at the tricritical point.

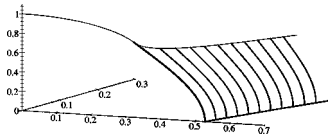


FIG. 2. Phase diagram of QCD with two light flavors of mass $m$ as calculated from the random matrix model. The almost parallel curves on the wing surface are cross sections of this surface with $m = \text{const}$ planes. The units of $m$ are $\sigma \approx 100$ MeV, of $T$ are $T_c \approx 160$ MeV, of $\mu$ are $\mu_1/0.53 \approx 2300$ MeV, with the choices of $T_c$ and $\mu_1$ from the text.

Away from the symmetry plane $m = 0$, the expressions for the wing surfaces and the wing lines become rather lengthy and will be presented elsewhere. The principle, however, remains simple. The minima of the potential $\Omega$ satisfy the equation $\partial\Omega/\partial\phi = 0$ and are given by (three out of five) roots of a fifth-order polynomial. On the wing surface, the depth $\Omega(\phi)$ in a pair of adjacent minima is the same. On the wing line, the two adjacent minima fuse into one. In terms of the roots of the polynomial, three roots coincide (two minima and one maximum). In other words, the potential is $\Omega \sim (\phi - \langle\phi\rangle)^4$ on the wing line and near the minimum.

The resulting phase diagram is plotted in Fig. 2. One can see, as expected from mean field theory near the tricritical point, that the wing lines together with the triple line approach the tricritical point with the same slope as the second-order line but from the other side. The critical exponents near the tricritical point as given by the random matrix model can be also seen coinciding, as expected, with the mean field exponents of Eqs. (15), (16), and (17).

From the random matrix model, we also learn how the zeros of the partition function in the complex $m$ plane evolve with changes in temperature and chemical potential. A few typical cases are illustrated in Fig. 3. At zero $T$ and $\mu$, the zeros form a cut (in the $N \to \infty$ limit) along imaginary axis. Raising the temperature pushes the zeros away from the origin along the imaginary axis until the density at the origin vanishes (continuously), the cut breaks in two, as in Fig. 3a, and chiral symmetry is restored [cf. Eq. (19)]. The chemical potential pushes the zeros away from the origin in the direction of the real axis until the cut splits in two, as illustrated in Fig. 3b. Note that the density $\rho(0)$ is finite just before the split. Therefore, the transition is of first order. Near the tricritical point, the split in the direction of the real axis (due to the chemical potential) occurs at the same time that the density $\rho(0)$ vanishes (due to the effects of the temperature). This is illustrated in Fig. 3c. The resulting dependence of

[6]With these values for $T_c$ and $\mu_1$, the parameters $a$ and $b$ have the values $a \approx 0.2$ and $b \approx 0.13$.

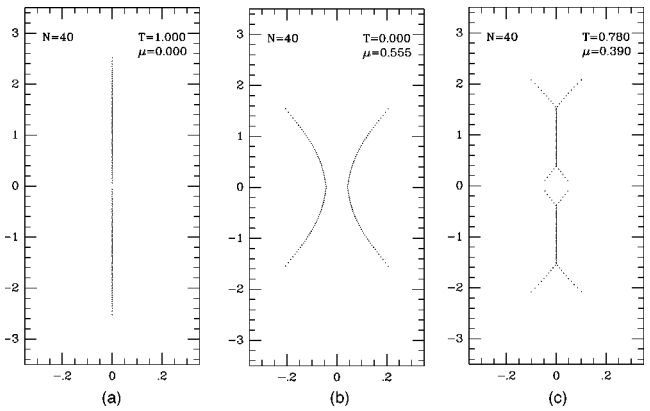


FIG. 3. Zeros of the partition function of a finite size $N$ random matrix model (20) in the complex $m$ plane calculated numerically at different values of $T$ and $\mu$. The calculation is done for $N_f=1$, but the $N\to\infty$ limit is $N_f$ independent. The density of points is proportional to the strength of the cut (discontinuity in $\langle\bar{\psi}\psi\rangle$) in the $N\to\infty$ limit.

$\langle\bar{\psi}\psi\rangle$ on $T$ and $\mu$ is shown in Fig. 4.

A comment should be added regarding the calculation of the baryon density $n$ in the random matrix model. The value of $(1/V_4)\partial \ln Z_{\rm RM}/\partial\mu$ does not represent the complete baryon density. The reason is that $\ln Z_{\rm RM}$ contains only contributions from the soft modes of the condensate, $\phi\sim\bar{\psi}\psi$. Further dependence on $\mu$ is contained in the contributions to $\ln Z$ from other degrees of freedom. In the effective Landau-Ginzburg theory, such additional contributions are embedded in the term $\Omega_0(T,\mu)$, Eq. (14). However, the *singular* behavior of the system is exclusively due to the soft modes of the condensate, i.e., terms involving $\phi$ in $\Omega_{\rm eff}$. Thus, it is legitimate to calculate singular properties of $n$, such as $\Delta n$, near a (tri)critical point using $(1/V_4)\partial \ln Z_{\rm RM}/\partial\mu$. At $T=0$, for example, we find

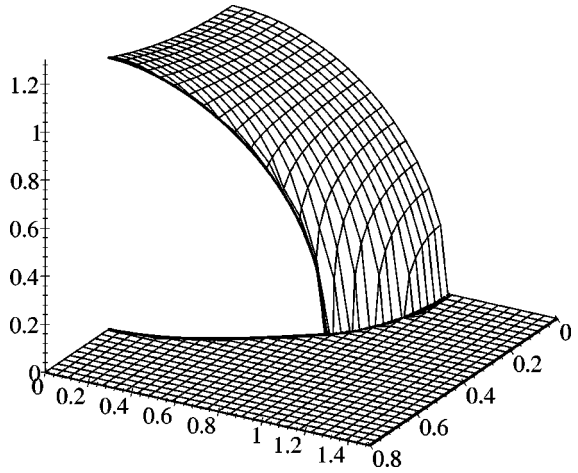

FIG. 4. The chiral condensate $\langle\bar{\psi}\psi\rangle$ (in units of $\langle\bar{\psi}\psi\rangle_0\approx 2\ {\rm fm}^{-3}$) as a function of $T$ and $\mu$ in the random matrix model. The units of $T$ and $\mu$ are the same as in Fig. 2.

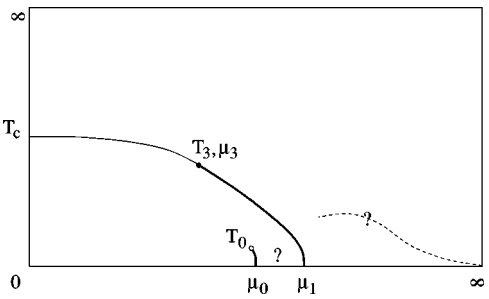


FIG. 5. A schematic phase diagram of QCD with 2 massless quark flavors. Other phase transition lines are possible, for example, in the low temperature region to the right of $\mu_0$. Another example is a transition associated with color superconductivity plotted as a dashed line. Thicker lines are first-order phase transitions. The $T_c-T_3$ line is a second-order phase transition. The tricritical point is at $T_3,\mu_3$ and the critical point of the nuclear matter liquid-gas transition is at $T_0$.

$$\Delta n V_4 = N\left[\left(\frac{\partial\Omega}{\partial\mu}\right)_{\phi=0} - \left(\frac{\partial\Omega}{\partial\mu}\right)_{\phi=\sqrt{1+\mu_1^2}}\right] = NN_f\left(\frac{2}{\mu_1}+2\mu_1\right)\approx 5NN_f, \tag{35}$$

in units of $1/\mu$, which is $b/N_c\Sigma$. With our previous choice of $\mu_1=1200$ MeV (i.e., $b\approx 0.13$), we find that $\Delta n\approx 0.4\ {\rm fm}^{-3}\approx 2.5 n_0$, which seems a reasonable estimate.

## VII. DISCUSSION AND SUMMARY

In this paper, we have presented an analysis (qualitative and, in some cases, quantitative) of the salient features of the phase diagram of QCD with two light or massless quark flavors at finite temperature and baryon chemical potential. The most important features of this phase diagram are summarized in Fig. 5. The phase diagram can certainly have a much richer structure. The phase transitions shown there are distinguished by the fact that a good order parameter can be associated with each of them. Here the term ''good order parameter'' implies the existence of some quantity whose expectation value is identically zero in some finite region of parameter space or in one phase and is some function of parameters in the other phase. Two such phases must be separated by a nonanalytic boundary, i.e. a phase transition. What is crucial here is the identical vanishing of an order parameter or its strict independence of the parameters of the theory. Usually, this is ensured by the existence of some symmetry with respect to which this order parameter transforms nontrivially.

For the chiral phase transition, a good order parameter is the value of $\langle\bar{\psi}\psi\rangle$, which spontaneously breaks the global $\mathrm{SU}(2)_L\times\mathrm{SU}(2)_R$ chiral symmetry to $SU(2)_V$. Hence, the phase with $\langle\bar{\psi}\psi\rangle=0$ and the phase with $\langle\bar{\psi}\psi\rangle\neq 0$ cannot be connected without crossing a phase transition line in the $T\mu$ plane.

The transition from $n\equiv 0$ to $n\neq 0$ along the $T=0$ line provides another example of a phase transition associated

with a good order parameter. The phases $n \equiv 0$ and $n \neq 0$ cannot be analytically connected; i.e. one must pass through a nonanalytic boundary (phase transition) when passing from one to the other. Since this is a first-order phase transition, continuity requires that there is also a first-order transition line for some $T \neq 0$. This line can, however, terminate since $n$ is no longer a good order parameter when $T \neq 0$.

The existence of a good order parameter is a sufficient but not a necessary condition for a phase transition. Other phase transition lines associated with more subtle phenomena are also possible. One interesting example, which attracted attention recently, is the transition associated with color superconductivity. The existence of a color superconducting phase was first argued for by Bailin and Love on the grounds that one gluon exchange is attractive in the color antitriplet quark-quark channel [14]. This means that the Fermi surface at very high $\mu$ becomes unstable and forms a gap. This phenomenon was recently reanalyzed using other methods at moderate values of $\mu$ with the conclusion that the effect is enhanced by instanton-induced interactions [16,15]. This means that another finite-$T$ transition, which stretches all the way to $\mu = \infty$, may be present on the phase diagram, Fig. 5.

This transition, unlike the chiral phase transition and the nuclear matter liquid-gas transition (at $T = 0$), does not seem to have a good order parameter associated with it. In particular, the diquark condensate $\langle \psi\psi \rangle$ is not gauge invariant. The dynamical mechanism responsible for the binding of diquark pairs is certainly operative at low temperatures, but the absence of a good order parameter does not allow us to assert that the temperature induced transition associated with the breaking of diquark pairs must always (i.e., at all $\mu$) proceed through a thermodynamic singularity rather than a smooth analytic crossover.

For some purposes, it is more natural to study the phase diagram in the space of density and temperature. The phase diagram of Fig. 5 can be converted into such a space and is shown in Fig. 6. A typical feature is that the first-order phase transition line from the $T\mu$ plane now appears as a region of phase coexistence in Fig. 6. In equilibrium, the values of density and temperature inside this region can be achieved only through an *inhomogeneous* mixture of two phases with different densities but the same $T$ and $\mu$. These densities are indicated by the ends of the horizontal lines drawn in the phase coexistence region.

The most interesting feature of the phase diagram of Figs. 5 and 6 is the presence of a tricritical point. Because of the fact that the critical dimensionality for such a point is equal to 3, critical behavior near this point is given by mean field theory plus logarithmic corrections. In particular, a simple random matrix model predicts the correct algebraic critical exponents.

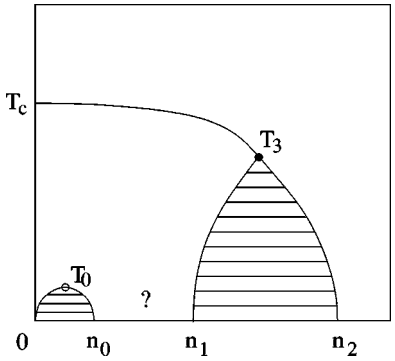


FIG. 6. The phase diagram of Fig. 5 shown as a function of density and temperature. The dashed line of the color superconductivity transition is not drawn. Horizontal lines connect points corresponding to densities of phases on two sides of the first-order line (i.e., the coexistence curve) of Fig. 5. The points $n_i$ on the $T = 0$ line are the same as on Fig. 1(a).

The tricritical point lies in the region expected to be probed by heavy ion collision experiments. It would be interesting to find an experimental signature for such a point. Since quark masses are not precisely zero, we should consider a slice of a three-dimensional phase diagram, Fig. 2, with $m \neq 0$. A qualitative difference between the phase diagram for $m \neq 0$ and that for $m = 0$ is the absence of the second-order phase transition line associated with the restoration of chiral symmetry. This symmetry is explicitly broken for $m \neq 0$. However, continuity from $m = 0$ ensures that the first-order finite density transition is still present at $m \neq 0$. This transition line is terminated by an ordinary critical point. Criticality at this point is not associated with chiral symmetry restoration, and excitations with the quantum numbers of pions do not become massless there. Criticality at this point is associated with the fact that a correlation length in the channel with the quantum numbers of the sigma meson becomes infinite. (Hence, it is plausible to infer that this point has the critical behavior of the three-dimensional Ising model.) Possible experimental signatures of this phenomenon are under investigation.

*Note added.* After this work was completed, a paper [42] appeared which addresses similar questions in the context of a Nambu–Jona-Lasinio model for color superconductivity. The results of [42] agree with and complement our findings.

## ACKNOWLEDGMENTS

Discussions with G. Brown, R. Pisarski, M. Prakash, K. Rajagopal, and E. Shuryak and a comment from M. Alford are greatly appreciated. This work was supported in part by DOE grant DE-FG-88ER40388 and NSF grant PHY-97-22101.

[1] HEMCGC and HTMCGC Collaborations, Nucl. Phys. B (Proc. Suppl.) **30**, 315 (1993).
[2] I. Barbour, N.-E. Behilil, E. Dagotto, F. Karsch, A. Moreo, M. Stone, and H. W. Wyld, Nucl. Phys. **B275** [FS17], 296 (1986).
[3] J. B. Kogut, M. P. Lombardo and D. K. Sinclair, Phys. Rev. D **51**, 1282 (1995); Nucl. Phys. B (Proc. Suppl.) **42**, 514 (1995).
[4] M. A. Stephanov, Phys. Rev. Lett. **76**, 4472 (1996).
[5] J. Stachel, Nucl. Phys. **A610**, 509c (1996).
[6] M. Asakawa and K. Yazaki, Nucl. Phys. **A504**, 668 (1989).
[7] A. Barducci, R. Casalbuoni, S. De Curtis, R. Gatto, and G. Pettini, Phys. Lett. B **231**, 463 (1989); Phys. Rev. D **41**, 1610

(1990); A. Barducci, R. Casalbuoni, G. Pettini, and R. Gatto, *ibid.* **49**, 426 (1994).
[8] N. Bilić, K. Demeterfi, and B. Petersson, Nucl. Phys. **B377**, 651 (1992).
[9] S. P. Klevansky, Rev. Mod. Phys. **64**, 649 (1992).
[10] G. E. Brown, M. Buballa, and M. Rho, Nucl. Phys. **A609**, 519 (1996).
[11] A. L. Fetter and J. D. Walecka, *Quantum Theory of Many-Particle Systems* (McGraw-Hill, New York, 1971).
[12] A. B. Migdal, E. E. Saperstein, M. A. Troitsky, and D. N. Voskresensky, Phys. Rep. **192**, 179 (1990).
[13] I. Klebanov, Nucl. Phys. **B262**, 133 (1985).
[14] D. Bailin and A. Love, Phys. Rep. **107**, 325 (1984).
[15] R. Rapp, T. Schäfer, E. V. Shuryak, and M. Velkovsky, Phys. Rev. Lett. **81**, 53 (1998).
[16] M. Alford, K. Rajagopal, and F. Wilczek, Phys. Lett. B **422**, 247 (1998).
[17] D. B. Kaplan and A. E. Nelson, Phys. Lett. B **175**, 57 (1986).
[18] E. Witten, Phys. Rev. D **30**, 272 (1984).
[19] E. Farhi and B. Jaffe, Phys. Rev. D **30**, 2379 (1984).
[20] L. P. Csernai and J. I. Kapusta, Phys. Rep. **131**, 223 (1986).
[21] W. Trautmann, in Dronten 1996, Correlations and clustering phenomena in subatomic physics; nucl-ex/9611002.
[22] R. Pisarski and F. Wilczek, Phys. Rev. D **29**, 338 (1984).
[23] F. Karsch and E. Laermann, Phys. Rev. D **50**, 6954 (1994); C. Bernard *et al.*, *ibid.* **54**, 4585 (1996); Phys. Rev. Lett. **78**, 598 (1997); Nucl. Phys. B (Proc. Suppl.) **63**, 400 (1998); Y. Iwasaki *et al.*, Phys. Rev. Lett. **78**, 179 (1997); S. Aoki *et al.*, Phys. Rev. D **57**, 3910 (1998).
[24] F. Brown *et al.*, Phys. Rev. Lett. **65**, 2491 (1990); Y. Iwasaki *et al.*, Phys. Rev. D **54**, 7010 (1996).
[25] I. D. Lawrie and S. Sarbach, in *Phase Transitions*, edited by C. Domb and J. L. Lebowitz (Academic, New York, 1984), Vol. 9, p. 1.
[26] E. V. Shuryak and J. J. M. Verbaarschot, Nucl. Phys. **A560**, 306 (1993).
[27] M. E. Berbenni-Bitsch, S. Meyer, A. Schafer, J. J. M. Verbaarschot, and T. Wettig, Phys. Rev. Lett. **80**, 1146 (1998).
[28] A. D. Jackson and J. J. M. Verbaarschot, Phys. Rev. D **53**, 7223 (1996).
[29] M. A. Stephanov, Phys. Lett. B **375**, 249 (1996).
[30] T. Wettig, A. Schäfer, and H. A. Weidenmuller, Phys. Lett. B **367**, 28 (1996).
[31] M. A. Halasz, A. D. Jackson, and J. J. M. Verbaarschot, Phys. Lett. B **395**, 293 (1997); Phys. Rev. D **56**, 5140 (1997).
[32] J. Feinberg and A. Zee, Nucl. Phys. **B504**, 579 (1997).
[33] R. A. Janik, M. A. Nowak, G. Papp, and I. Zahed, Acta Phys. Pol. B **28**, 2949 (1997).
[34] T. Banks and A. Casher, Nucl. Phys. **B169**, 103 (1980).
[35] A. D. Jackson, M. K. Sener and J. J. M. Verbaarschot, Nucl. Phys. **B479**, 707 (1996).
[36] C. N. Yang and T. D. Lee, Phys. Rev. **87**, 104 (1952); T. D. Lee and C. N. Yang, **87**, 410 (1952).
[37] E. Brézin, S. Hikami, and A. Zee, Nucl. Phys. **B464**, 411 (1996).
[38] G. Akemann, P. Damgaard, U. Magnea, and S. Nishigaki, Nucl. Phys. **B487**, 721 (1997).
[39] T. Guhr and T. Wettig, Nucl. Phys. **B506**, 589 (1997).
[40] Y. V. Fyodorov, M. Titov, and H.-J. Sommers, cond-mat/9802306.
[41] E. V. Shuryak, Nucl. Phys. **B203**, 93 (1982).
[42] J. Berges and K. Rajagopal, hep-ph/9804233.